Raman lidar measurements of aerosol and water vapour distribution in the atmosphere: A novel method of signal processing

N Sangeetha[1], Bhavani Kumar Yellapragada[2], S.Sivabalan[3]

[1] School of Electronics Engineering, VIT University, Vellore-632014, Tamil Nadu, India,
Email:nsangeetha@vit.ac.in
[2]National Atmospheric Research Laboratory, ISRO, Gadanki-517112, India,
Email: ypbk@narl.gov.in
[3]School of Electrical Engineering, VIT University, Vellore-632014, Tamil Nadu, India,
Email:ssivabalan@vit.ac.in

Key words: Raman lidar, photon counting, scaled analog, dead-time correction, gluing method.

ABSTRACT: Raman lidar is one of the active remote sensors of atmospheric water vapour. This method also provides reliable information on microphysical parameters of aerosol particles in the atmosphere. Raman lidar uses elastic and inelastic backscatter to derive the profiles of key atmospheric parameters. The prime advantage of this method is the direct determination of particle backscatter and extinction coefficients along with atmospheric water vapor simultaneously. The optical part of lidar system employs a set of wavelength separating mirrors and high-spectral-resolution interference filters to separate the vibrational Raman signals from the strong elastic backscattering signal. Since Raman signal strengths are weak in nature than compared to the elastic, the detected signals need to be recorded using a unique data acquisition system. The special data acquisition system uses both analog and photon counting electronics, which allows enhanced dynamic range in the measured signals. In order to achieve the enhancement in measured profiles, a gluing technique is required to apply between the signals of analog and photon counting. This paper presents an efficient gluing algorithm to retrieve the profiles of elastic and Raman signals from the functional Raman lidar.

1. INTRODUCTION

Atmospheric research is currently hard to envisage without making use of remote-sensing techniques. Water vapor is the most imperative gas in the atmosphere because, it is an active absorber of infrared (IR) radiation and also the most significant greenhouse gas in the atmosphere. Water vapor is strongly influences the radiation budget of the atmosphere by its impact on cloud formation. Depending on the location in the atmosphere, water vapour affects the radiative balance by reflecting incoming solar radiation. Further, the significant components of atmosphere which affects the radiation budget are aerosols. Aerosols are small particles that suspend in the atmosphere with dynamic characteristic and influence the climate in different ways. They also increase the absorption and scattering of solar radiation, hence this phenomena directly impact the atmospheric radiation budget. Aerosols are act as cloud condensation nuclei in cloud droplet formation, therefore, they have an indirect effect on the radiation budget of the atmosphere by moderating cloud formation process and cloud droplet optical properties. Atmospheric aerosols arise from different sources such as anthropogenic, human – made, fossil fuel combustion, forest fire, dust come from the earth surface, volcanoes, and other sources (Turner et al. 2002).

Light detection and ranging (lidar) is one of the important techniques in profiling the atmosphere. The lidar provides high spatial and temporal resolution of the measurements and potential coverage of the altitude range from the ground to more than 100 Km. The emitted laser radiation into the atmosphere performs a variety of interaction processes with the atmospheric constituents, which in turn used to determine the basic atmospheric variable ssuch as pressure, temperature, humidity, wind, aerosols, trace gases and clouds (Wandinger, 2005). Raman lidar is one among the types of lidar, which works on the base of Raman effect, it is a discovery of C V Raman about a very weak type of secondary light that is generated at wavelengths shifted from the incident wavelength. This phenomenon is utilized for characterizing the chemical identity of the scatterer because, the frequency shifts are unique to the substance causes the scattering. When atmosphere is illuminated with a laser light, the frequency shifted backscattered radiation of the Raman components can be obtained. Raman lidars can collect the vibrational Raman backscattered returns of the atmospheric constituents like oxygen (O_2), Nitrogen (N_2) and water vapor molecules (H_2O) using the above mentioned technique (Weitkamp, 2006, Whiteman et al. 1992.). Raman with Elastic lidar deployed in National Atmospheric Research Lab (NARL) is developed indigenously and demonstrated successfully. This ground based lidar has an elastic channel at 355 nm wavelength and nitrogen and water vapor at 387 nm and 408 nm respectively, which remote sense the atmospheric water vapor and aerosols in the boundary layer (Yellapragada, 2016).

Photoelectric detection is a vital process in the receiving system of the lidar. Since the dynamic range of the received signal is very large for a ground based lidar, both photon counting (PC) and analog-to-Digital (AD) modes are used to cover the entire dynamic range in various lidar system.AD can convert analog voltage into digital signal with superior linearity in near-field range, however it cannot detect weak signal from far field effectively. In contrast, PC mode can efficiently detect the far-field signal by counting the pulses produced by the single photon. But the intensity of the near-field signal can easily exceed the maximum counting rate of PC, which eventually saturates the photon counting rate. This results in nonlinear error in PC signal. Therefore, AD and PC signals should be joined into one single profile to detect the near and far filed signals independently (Whiteman et al. 2006).

The gluing algorithm is one of the important requirements to be considered for enhancing the measurement correctness in the atmospheric parameters (Zhi-Shen Liu et al. 2009, Petty et al. 2006). The methods that are widely used for gluing AD and PC signals are curve fitting and linear regression (Newsom et al. 2009). In this paper, we propose a gluing method which finds the regression coefficients from original AD and PC signal, which is then used to converts the analog data into PC counts. Further, the dead-time of the detector is corrected in PC signals in order to avoid the overlapping of photon counts. At last the gluing algorithm is applied and glued the AD and PC signals.

2. METHODOLOGY

In lidar systems, high dynamic range photomultiplier tubes (PMT) are used to detect the backscattered light from the atmosphere and the output analog voltage signal is converted into digital signal by AD converter or the output signal is converted into photon counts by photon converter. In addition, these digital and analog signals must be glued to retrieve the raw data. The gluing process of AD and PC data is shown in the Figure 1. The glued signal is calculated from the converted AD and PC by applying the gluing algorithm. At first, the algorithm starts by separating original AD and PC data from one minute data and then the same process is repeated for ~ 2 hours data retrieved from the Raman Lidar (Gadanki 02/01/2015, 18:31:26 to 20:28:47). Secondly, Dead-time correction is carried out with the original PC data. In the process of detection, the photon counting (PC) takes a time to record the backscattered light after every event during which the system is not able to record an another event which is called as dead time. However, the Licel photon counter employed in the lidar system is a non- paralyzable detector, where an event happening during the dead time is completely lost. Because of that, with an increasing event rate, the detector reaches a saturation rate which is equal to that of inverse of the dead time. The Photon Counter used in lidar system has dead time of 4ns. The equation of the non-paralyzable system is expressed as (Fuyi et al. 2013):

$$N_{true} = \frac{N_{obs}}{1-N_{obs}*\tau_d} \qquad \text{---------- (1)}$$

Where, N_{true} = The observed count rate; N_{obs} = The true count rate

τ_d = The system dead time

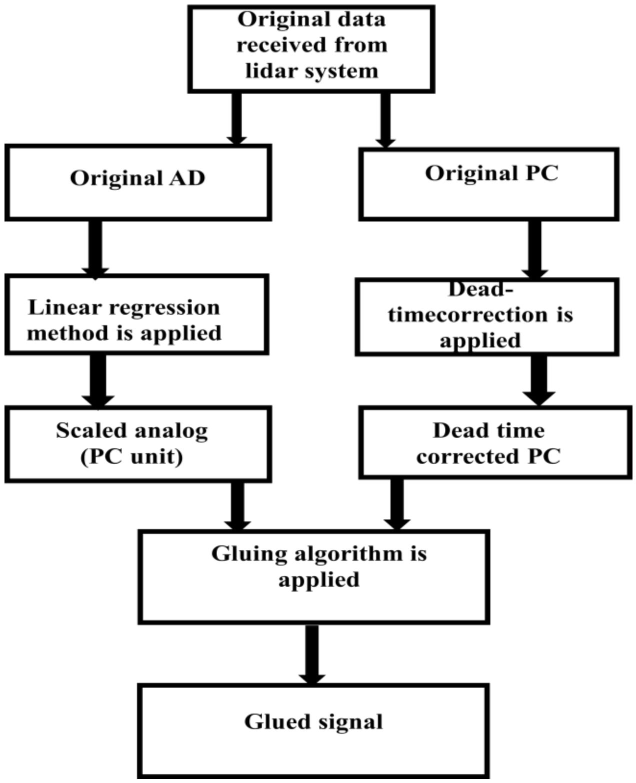

Figure 1. Flow chart illustrating the gluing of PC and AD data

Thirdly, the gluing algorithm equation (2) is applied to calculate the scaled analog signal. The Linear regression coefficients a and b were applied to the analog signal to convert them to photon unit (from mV into counts). After the conversion, a new signal named scaled analog is obtained. The gluing algorithm equation is represented as

$$\sum_{i=1}^{n}(PC(z_i) - (a * Analog\ (z_i) + b))^2 = min \qquad \text{---------- (2)}$$

Here, z_i represents the altitude of the profile. The valid region of gluing of both the signals is between 0.5 MHz (lower toggle rate) and10 MHz (upper toggle rate). However, above 10 MHz, scaled analog is used or if toggle rate is less than 0.5 MHz, photon counting data is used. In principle one should glue two signals only if the following scenarios occur.

1. The peak value of the dead – time corrected photon counting is above the maximum toggle rate
2. The background of the dead-time corrected photon counting is below the minimum toggle rate.
   These gluing strategies are verified in our gluing process.

3. RESULTS AND DISCUSSION

The data used in this paper was obtained from functional lidar system at NARL. The data is the original signal profiled during the night time for two hours. The original data that is retrieved from the data acquisition system is then converted into ASCII format. The ASCII data implies the AD and PC data of backscattered (355 nm) light, nitrogen (387 nm) and water vapor (408 nm), for 60 Km of range in atmosphere which is equivalent to 2000 bins. Here, AD data is retrieved from each 30 m bins and PC data is retrieved from each 240 m bins. Since the number bins of PC data is less than the AD, the interpolation has to be applied to PC signal in order to synchronize with the AD data. This should be done for all the wavelengths and enhanced gluing algorithm is applied for each wave length.

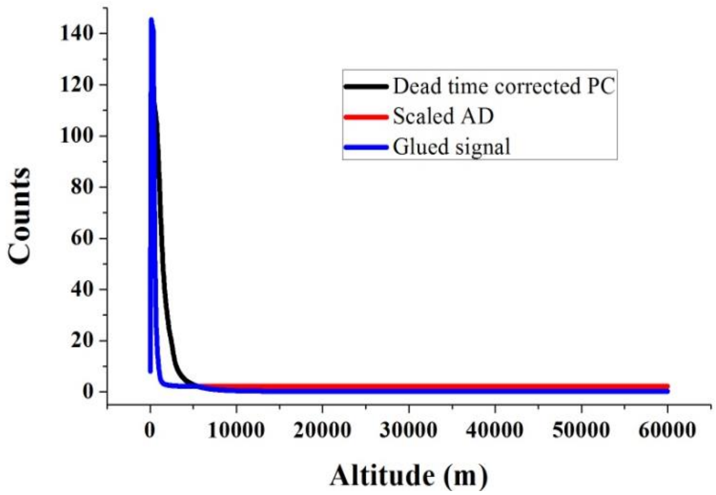

Figure 2. Dead-time corrected PC (black), Scaled analog signal (red), and glued signal (blue) of 355 nm backscattered signal up to 60 Km of altitude.

Figure 2 shows the dead time corrected PC, scaled analog AD, and glued signal of both AD and PC for 355 nm backscattered signal. It can be seen that the scaled analog signal reaches 146 counts peak at 120 meters, and the dead time corrected PC reaches the 115 counts peak at 30 meters. Using the gluing algorithm in equation (2), the minimum point is found at 5490 meters of altitude. Therefore, the transition point between photon dead time corrected and scaled analog is 5490 m (i.e., 5.49 Km). This altitude is exactly in the suitable range for gluing AD and PC signals. The resulting glued signal shown in Figure 3. It is clear from the figure that, the scaled analog is absent beneath the altitude of 5.49 Km, since, it is completely replaced by the dead time corrected PC signals. This signal is called glued signal which provides the AD signal at near- field which gives good linearity to the profiles of various wavelength. On the other hand, the far-field utilizes the PC signal as it is weak at near-field.

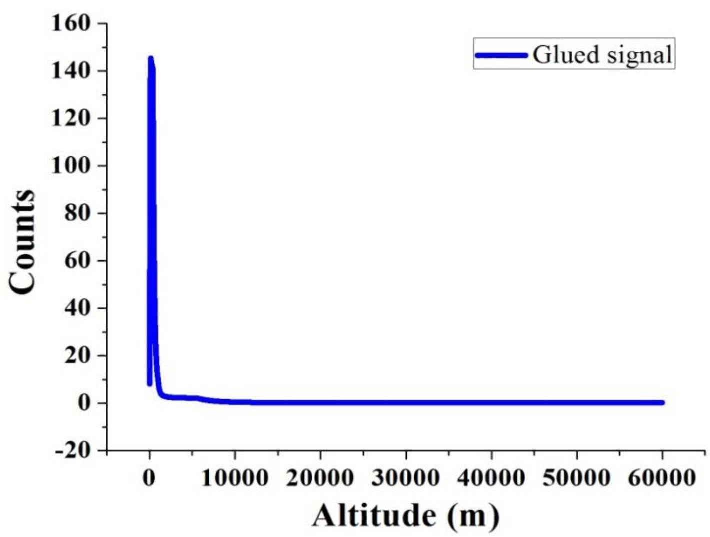

Figure 3.Glued signal profile of 355 nm backscattered signal for 60 Km.

Figure.4 shows the dead time corrected PC, scaled analog AD, and glued signal details up to 10 Km of altitude for 355 nm wavelength. Saturation of PC signal occurs from 5.49 Km, which is highlighted (green) in the plot. The glued signal is consistent with AD at lower altitudes (up to 5.49 Km) and it is consistent with PC from 5.49 Km to higher altitudes. However, the glued signal corrects the saturation of PC signal by gluing process.

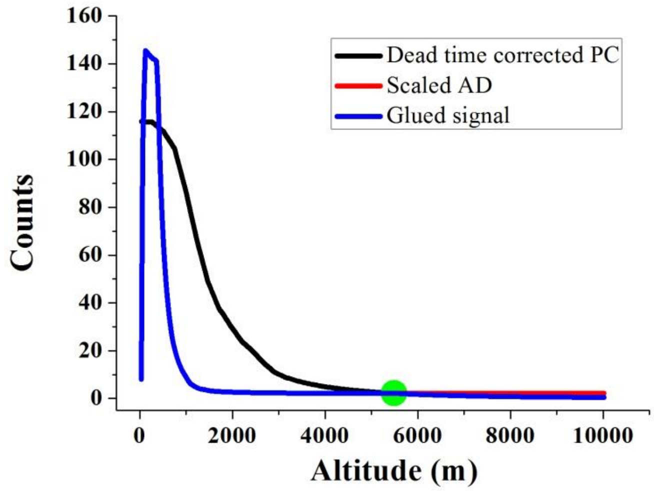

Figure 4. Dead-time corrected PC (black), Scaled analog signal (red), and glued signal (blue) of 355 nm backscattered signal up to 10 Km of altitude.

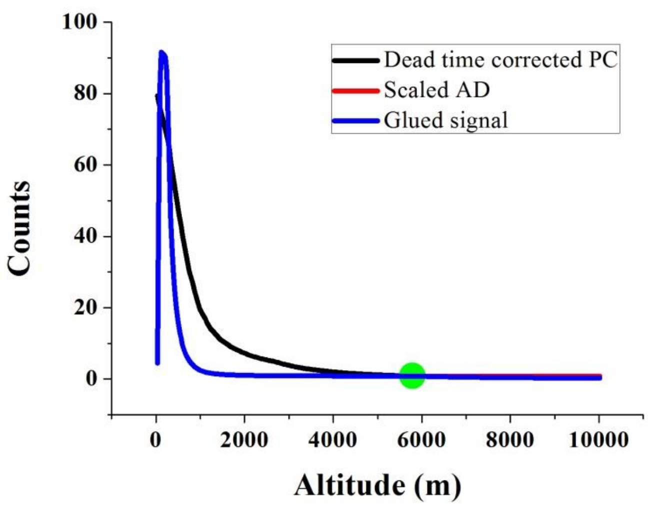

Figure 5. Dead-time corrected PC (black), Scaled analog signal (red), and glued signal (blue) of 387 nm nitrogen signal up to 10 Km of altitude.

Figure 5 shows the resulting graph of enhanced gluing algorithm applied to the nitrogen signal at 387 nm of wavelength. It can be seen that, the peak signal of AD occurs at 91 counts in 120 metres of altitude. This is also the peak of glued signal. The dead time corrected PC signal peaks at 91 counts in 30 metres of altitude. According to the gluing algorithm in equation (2), the minimum point is found at 5760 meters of altitude. Therefore, the transition point between photon dead time corrected and scaled analog is 5760 m (i.e., 5.76 Km). This is highlighted (green) in the graph. However, this altitude is the suitable range for gluing AD and PC signals of nitrogen signal.

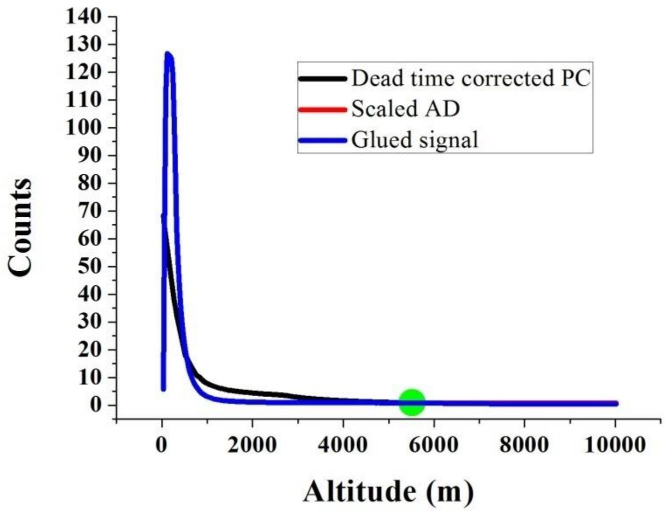

Figure 6. Dead-time corrected PC (black), Scaled analog signal (red), and glued signal (blue) of 408 nm water vapor signal up to 10 Km of altitude.

Figure 6 is the subsequent graph of enhanced gluing algorithm realised to the water vapor signal at 408 nm of wavelength. It can be seen that, the peak signal of AD occurs at 126 counts in 120 metres of altitude. This is also the peak of glued signal of water vapor. The dead time corrected PC signal peaks at 68 counts in 30 metres of altitude. According to the gluing algorithm, the minimum point is found at 5520 meters of altitude, which is significant for water vapour signals. Therefore, the transition point between photon dead time corrected and scaled analog is 5520 m (i.e., 5.20 Km) for 408 nm signal. This is highlighted (green) in the graph. However, this altitude is the suitable range for gluing AD and PC signals of water vapor signal.

4. CONCLUSION

The enhanced gluing algorithm for combining AD and PC signals of a functional Raman lidar system is proposed and verified in this paper. The proposed algorithm is executed using MATLAB platform and the respective flowchart is discussed. The scaled AD and the dead time corrected PC profiles of 355 nm of backscattered signal, 387 nm of nitrogen signal and 408 nm of water vapour signals are presented. The glued profile of the respective signals for different altitude are graphically plotted and discussed.

5. REFERENCE

Fuyi, T., Abdullah, K., Lim, H.S., MatJafri, M.Z., Welton, E.J. and Lolli, S., 2013, July. An initial assessment of ground based lidar backscattered signal in Penang Island. In *Space Science and Communication (IconSpace)*, pp. 228-232.

Liu, Z., Li, Z., Liu, B. and Li, R., 2009. Analysis of saturation signal correction of the troposphere lidar. *Chinese Optics Letters*, *7*(11), pp.1051-1054.

Newsom, R.K., Turner, D.D., Mielke, B., Clayton, M., Ferrare, R. and Sivaraman, C., 2009. Simultaneous analog and photon counting detection for Raman lidar. *Applied Optics*, *48*(20), pp.3903-3914.

Petty, D. and Turner, D., 2006, July. Combined analog-to-digital and photon counting detection utilized for continuous Raman lidar measurements. In *Proceedings of the 23rd International Laser Radar Conference, post deadline paper* .Vol. 7574.

Turner, D.D and Whiteman, D.N., 2002. Remote Raman Spectroscopy.Profiling Water VaporandAerosols in the Troposphere Using Raman Lidars. *Handbook of Vibrational Spectroscopy, edited by* John M. Chalmers and Peter R. Griffiths , John Wiley & Sons Ltd, Chichester, pp.1-19.

Wandinger, U., 2005. Introduction to Lidar in Lidar-Range-Resolved Optical Remote Sensing of the Atmosphere. *Springer, New York*.pp.1-18.

Weitkamp, C. ed., 2006. *Lidar: range-resolved optical remote sensing of the atmosphere* (Vol. 102). Springer Science & Business,pp.241-267.

Whiteman, D.N., Melfi, S.H. and Ferrare, R.A., 1992. Raman lidar system for the measurement of water vapor and aerosols in the Earth's atmosphere. *Applied Optics*, *31*(16), pp.3068-3082.

Whiteman, D.N., Demoz, B., Rush, K., Schwemmer, G., Gentry, B., Di Girolamo, P., Comer, J., Veselovskii, I., Evans, K., Melfi, S.H. and Wang, Z., 2006. Raman lidar measurements during the International H2O Project. Part I: Instrumentation and analysis techniques. *Journal of Atmospheric and Oceanic Technology*, *23*(2), pp.157-169.

Yellapragada, B.K., 2016. Lidar research activities and observations at NARL site, Gadanki, India. In: *SPIE Asia-Pacific Remote Sensing* , International Society for Optics and Photonics. pp. 98790S-98790S.